

A Map-Reduce Parallel Approach to Automatic Synthesis of Control Software

Vadim Alimghuzin^{1,2}, Federico Mari¹, Igor Melatti¹, Ivano Salvo¹, and Enrico Tronci¹

¹ Computer Science Department, Sapienza University of Rome, Italy,
 {alimghuzhin,mari,melatti,salvo,tronci}@di.uniroma1.it.

² Department of Computer Science and Robotics, Ufa State Aviation Technical University,
 Russian Federation.

Abstract. Many Control Systems are indeed Software Based Control Systems, i.e. control systems whose controller consists of control software running on a microcontroller device. This motivates investigation on Formal Model Based Design approaches for automatic synthesis of control software.

Available algorithms and tools (e.g., *QKS*) may require weeks or even months of computation to synthesize control software for large-size systems. This motivates search for parallel algorithms for control software synthesis.

In this paper, we present a map-reduce style parallel algorithm for control software synthesis when the controlled system (*plant*) is modeled as discrete time linear hybrid system. Furthermore we present an MPI-based implementation *PQKS* of our algorithm. To the best of our knowledge, this is the first parallel approach for control software synthesis.

We experimentally show effectiveness of *PQKS* on two classical control synthesis problems: the inverted pendulum and the multi-input buck DC/DC converter. Experiments show that *PQKS* efficiency is above 65%. As an example, *PQKS* requires about 16 hours to complete the synthesis of control software for the pendulum on a cluster with 60 processors, instead of the 25 days needed by the sequential algorithm in *QKS*.

1 Introduction

Many Embedded Systems are indeed Software Based Control Systems (SBCSs). An SBCS consists of two main subsystems: the controller and the plant. Typically, the plant is a physical system consisting, for example, of mechanical or electrical devices whereas the controller consists of control software running on a microcontroller. In an endless loop, at discrete time instants (sampling), the controller after an Analog-to-Digital (AD) conversion (quantization), reads sensor outputs from the plant and after a Digital-to-Analog (DA) conversion, sends commands to plant actuators. The controller selects commands in order to guarantee that the closed-loop system (that is, the system consisting of both plant and controller) meets given safety and liveness specifications (System Level Formal Specifications).

Software generation from models and formal specifications forms the core of Model Based Design of embedded software [1]. This approach is particularly interesting for SBCSs since in such a case system level (formal) specifications are much easier to define than the control software behavior itself.

1.1 Motivations

In [2] it is presented an algorithm, along with a tool *QKS*, that returns correct-by-construction control software starting from the following specifications: i) a formal model of the controlled system, modeled as a Discrete Time Linear Hybrid System (DTLHS), ii) safety and liveness requirements (goal region) and iii) number b of bits for AD conversion.

To this aim, in *QKS* first computes a suitable finite discrete abstraction (*control abstraction* [2]) $\hat{\mathcal{H}}$ of the DTLHS plant model \mathcal{H} , where $\hat{\mathcal{H}}$ depends on the quantization schema (i.e. number of bits b needed for AD conversion) and it is the plant as it can be seen from the control software after AD conversion. Then, given an abstraction \hat{G} of the goal states G , it is computed a controller \hat{K} that starting from any initial abstract state, drives $\hat{\mathcal{H}}$ to \hat{G} regardless of possible nondeterminism. Control abstraction properties ensure that \hat{K} is indeed a (quantized representation of a) controller for the original plant \mathcal{H} . Finally, the finite automaton \hat{K} is translated into control software (C code). The whole process is summarized in Fig 1.

While effective on moderate-size systems, *QKS* computation time is exponential in b , thus resulting in a bottleneck when synthesizing controllers for larger systems. This motivates search of parallel versions of *QKS* synthesis algorithm. In fact, from a computational point of view, the most critical step of *QKS* is the control abstraction $\hat{\mathcal{H}}$ generation (which is responsible for more than 95% of the overall computation, see [2]). This stems from the fact that $\hat{\mathcal{H}}$ is computed explicitly, by solving a Mixed Integer Linear Programming (MILP) problem for each triple $(\hat{x}, \hat{u}, \hat{x}')$ (where \hat{x}, \hat{x}' are abstract states of $\hat{\mathcal{H}}$ and \hat{u} is an abstract action of $\hat{\mathcal{H}}$). Since the number of abstract states is 2^b , being b the number of bits needed for AD conversion of all variables in the plant, we have that *QKS* computation time is exponential in $2b + b_u$ (being b_u the number of bits needed to encode actions). In *QKS* suitable optimizations reduce the complexity to be exponential in $b + b_u$. However, for large-sized system this may lead to unacceptable computation time, even considering that the finite state abstraction generation is an off-line computation. In large-sized embedded systems this computation may take up to weeks or even months since b may be very large for two typical reasons. First, since each plant continuous state variable needs to be quantized, the number of bits is necessarily high when the plant model consists of many continuous variables, such as, for example, in an air traffic control system [3]. Second, controllers synthesized by considering a finer quantization schema usually have a better behaviour with respect to non-functional requirements, such as *ripple* and *set-up time*. Therefore, when a high precision is required, a small sampling time and a large number of quantization bits must be considered.

As an example, experimental results show that *QKS* takes nearly one month (25 days) of CPU time to synthesize the controller for a 13 bits quantized inverted pendulum (which is described by only two continuous state variables, see Sect. 5.1). Moreover, 99% of those 25 days of computation is devoted to control abstraction generation. This may result in a loss in terms of time-to-market in control software design when *QKS* is used.

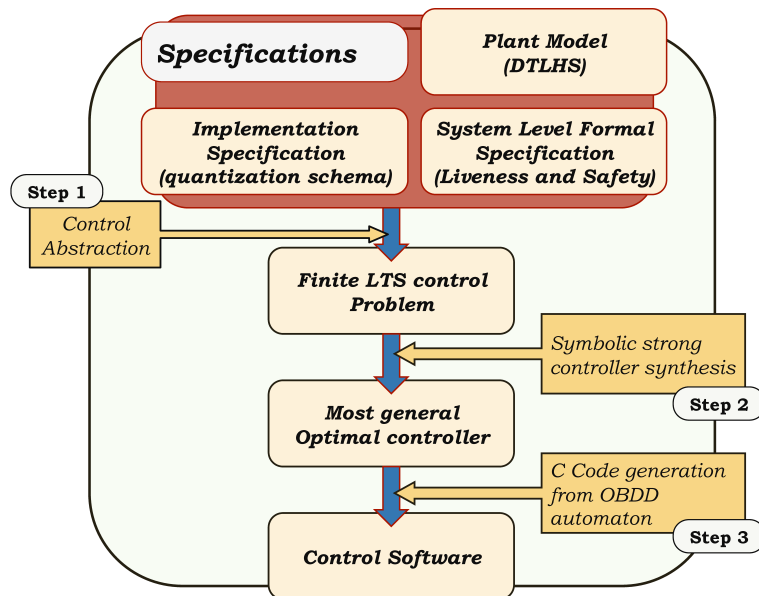


Fig. 1. Control Software Synthesis Flow.

1.2 Main Contributions

To overcome such obstruction, in this paper we show that the *QKS* control abstraction procedure may be organized as an embarrassingly parallel task. Map-Reduce [4] is a (LISP inspired) programming paradigm advocating a form of *embarassing parallelism* for effective massive parallel processing. An implementation of such an approach is in Hadoop (e.g., see [5]). The effectiveness of the Map-Reduce approach stems from the minimal communication overhead of *embarassing parallelism*. This motivates our goal of looking for a map-reduce style parallel algorithm for control software synthesis from system level. Hence, we design a parallel version of *QKS*, that is inspired to the map-reduce programming style and that we call *Parallel QKS* (*PQKS* in the following). *PQKS* is actually implemented using MPI (Message Passing Interface) and it is designed to exploit the computational power available in modern computer clusters (distributed memory model). Such an algorithm will be presented in Sect. 4, after a discussion of the basic notions needed to understand our approach (Sects. 2) and the description of the standalone (i.e. serial) algorithm of *QKS* (Sect. 3).

We assess the effectiveness of *PQKS* by running it on two widely used embedded system, which are challenging examples for the automatic synthesis of correct-by-construction control software: the multi-input buck DC-DC converter [6] and the inverted pendulum [7] benchmarks. Namely, experimental results on the above described benchmarks will be discussed in Sect. 5, also showing that we achieve a nearly linear speedup w.r.t. *QKS*, with efficiency above 65%. As an example, *PQKS* requires about 16 hours to complete the above mentioned synthesis of the 13-bits pendulum on a cluster with 60 processors, instead of the 25 days of *QKS*.

1.3 Related Work

In the literature there are many works presenting algorithms (and tools) for the automatic synthesis of control software under various assumptions. As an example, the works in [8,9,10,7] propose algorithms expressing the input model in discrete time and are able to manage infinite-state systems like those arising from hybrid systems, our focus here. However, no one of such approaches has a parallel version of any type, thus the algorithms they propose suffer of the same bottleneck as *QKS*.

A parallel algorithm for control software synthesis has been presented in [11], where however non-hybrid systems are addressed, control is obtained by Monte Carlo simulation and quantization is not taken into account. Moreover, note that in literature “parallel controller synthesis” often refers to synthesizing parallel controllers (e.g., see [12] and [13] and citations thereof), whilst here we parallelize the (offline) computation required to synthesize a standalone controller.

As discussed in Sect. 1.1, the present paper builds mainly upon the tool *QKS* presented in [2]. Other works about *QKS* comprise the following ones. In [14] it is shown that expressing the input system as a linear predicate over a set of continuous as well as discrete variables is not a limitation on the modeling power. In [15] it is shown how non-linear systems may be modeled by using suitable linearization techniques. The paper in [16] addresses model based synthesis of control software by trading system level non-functional requirements (such as optimal set-up time, ripple) with software

non-functional requirements (its footprint, i.e. size). The procedure which generates the actual control software (C code) starting from a finite automaton of a control law is described in [17]. In [18] it is shown how to automatically generate a picture illustrating control software coverage. Finally, in [19] it is shown that the *quantized control synthesis problem* underlying QKS approach is undecidable. As a consequence, QKS is based on a correct but non-complete algorithm. Namely, QKS may return one of the following results: i) SOL, in which case a correct-by-construction control software is returned; ii) NOSOL, in which case no controller exists for the given specifications; iii) UNK, in which case QKS was not able to compute a controller, but a controller may exist.

Summing up, to the best of our knowledge, no previous *parallel* control software synthesis from formal specifications has been published.

2 Background on DTLHS Control Software Synthesis

To make this paper self-contained, in this section we briefly summarize previous work on automatic generation of control software for *Discrete Time Linear Hybrid System* (DTLHS) from System Level Formal Specifications.

As shown in Fig. 1, we model the controlled system (i.e. the plant) as a DTLHS (Sect. 2.4), that is a discrete time hybrid system whose dynamics is modeled as a *guarded (linear) predicate* (Sect. 2.1) over a set of continuous as well as discrete variables. The semantics of a DTLHS is given in terms of a *Labeled Transition Systems* (LTS, Sect. 2.2). Given a DTLHS plant model \mathcal{H} , a set of *goal states* G (*liveness specifications*) and an *initial region* I , both represented as linear predicates, we are interested in finding a *restriction* K of the behaviour of \mathcal{H} such that in the *closed loop system* all paths starting in a state in I lead to G after a finite number of steps. Finding K is the DTLHS *control problem* (Sect. 2.5) that is in turn defined as a suitable LTS control problem (Sect. 2.3). Since we want to output a control software, we are interested in controllers that take their decisions by looking at *quantized states*, i.e. the values that the control software reads after an AD conversion. To this aim, the solution of a *quantized control problem* (Sect. 2.6) is computed by first generating a discrete abstraction of \mathcal{H} , called *control abstraction* (Sect. 3, step 1 in Fig. 1), then by applying to such control abstraction known techniques in order to generate a controller (step 2 in Fig. 1), and finally synthesizing a control software (step 3 in Fig. 1). Our main contribution in this paper is in the control abstraction generation, thus we will focus this section on the basic notions to understand definition and computation of control abstractions (Sect. 3).

2.1 Predicates

We denote with $[n]$ an initial segment $\{1, \dots, n\}$ of the natural numbers. We denote with $X = [x_1, \dots, x_n]$ a finite sequence of variables that we may regard, when convenient, as a set. Each variable x ranges on a known (bounded or unbounded) interval \mathcal{D}_x either of the reals (continuous variables) or of the integers (discrete variables). We denote with \mathcal{D}_X the set $\prod_{x \in X} \mathcal{D}_x$. Boolean variables are discrete variables ranging on the set $\mathbb{B} = \{0, 1\}$. To clarify that a variable x is *continuous* (resp. *discrete*, resp. *boolean*)

we may write x^r (resp. x^d, x^b). Analogously X^r (X^d, X^b) denotes the sequence of real (discrete, boolean) variables in X . Unless otherwise stated, we suppose $\mathcal{D}_{X^r} = \mathbb{R}^{|X^r|}$ and $\mathcal{D}_{X^d} = \mathbb{Z}^{|X^d|}$. If x is a boolean variable, we write \bar{x} for $(1 - x)$.

A *linear expression* over a list of variables X is a linear combination of variables in X with rational coefficients. A *linear constraint* over X (or simply a *constraint*) is an expression of the form $L(X) \leq b$, where $L(X)$ is a linear expression over X and b is a rational constant. In the following, we also write $L(X) \geq b$ for $-L(X) \leq -b$.

Predicates are inductively defined as follows. A constraint $C(X)$ over a list of variables X is a predicate over X . If $A(X)$ and $B(X)$ are predicates over X , then $(A(X) \wedge B(X))$ and $(A(X) \vee B(X))$ are predicates over X . Parentheses may be omitted, assuming usual associativity and precedence rules of logical operators. A *conjunctive predicate* is a conjunction of constraints. For conjunctive predicates we will also write: $L(X) = b$ for $((L(X) \leq b) \wedge (L(X) \geq b))$ and $a \leq x \leq b$ for $x \geq a \wedge x \leq b$, where $x \in X$.

Given a constraint $C(X)$ and a fresh boolean variable (*guard*) $y \notin X$, the *guarded constraint* $y \rightarrow C(X)$ (if y then $C(X)$) denotes the predicate $((y = 0) \vee C(X))$. Similarly, we use $\bar{y} \rightarrow C(X)$ (if not y then $C(X)$) to denote the predicate $((y = 1) \vee C(X))$. A *guarded predicate* is a conjunction of either constraints or guarded constraints.

2.2 Labeled Transition Systems

A *Labeled Transition System* (LTS) is a tuple $\mathcal{S} = (S, \mathcal{A}, T)$ where S is a (possibly infinite) set of states, \mathcal{A} is a (possibly infinite) set of actions, and $T : S \times \mathcal{A} \times S \rightarrow \mathbb{B}$ is the *transition relation* of \mathcal{S} . We say that T (and \mathcal{S}) is *deterministic* if $T(s, a, s') \wedge T(s, a, s'')$ implies $s' = s''$, and *nondeterministic* otherwise. Let $s \in S$ and $a \in \mathcal{A}$. We denote with $\text{Adm}(\mathcal{S}, s)$ the set of actions admissible in s , that is $\text{Adm}(\mathcal{S}, s) = \{a \in \mathcal{A} \mid \exists s' : T(s, a, s')\}$ and with $\text{Img}(\mathcal{S}, s, a)$ the set of next states from s via a , that is $\text{Img}(\mathcal{S}, s, a) = \{s' \in S \mid T(s, a, s')\}$. We call *self-loop* a transition of the form $T(s, a, s)$. A *run* or *path* for an LTS \mathcal{S} is a sequence $\pi = s_0, a_0, s_1, a_1, s_2, a_2, \dots$ of states s_t and actions a_t such that $\forall t \geq 0 \ T(s_t, a_t, s_{t+1})$. The length $|\pi|$ of a finite run π is the number of actions in π . Sometimes s_t (resp. a_t) will be denoted by $\pi^{(S)}(t)$ (resp. $\pi^{(A)}(t)$).

2.3 LTS Control Problem and Solutions

A *controller* for an LTS \mathcal{S} is used to restrict the dynamics of \mathcal{S} so that all states in the initial region will reach the goal region. In the following, we formalize such a concept by defining solutions to an LTS control problem. In what follows, let $\mathcal{S} = (S, \mathcal{A}, T)$ be an LTS, $I, G \subseteq S$ be, respectively, the *initial* and *goal* regions of \mathcal{S} .

Definition 1. A controller for \mathcal{S} is a function $K : S \times \mathcal{A} \rightarrow \mathbb{B}$ such that $\forall s \in S, \forall a \in \mathcal{A}$, if $K(s, a)$ then $\exists s' \ T(s, a, s')$. If $K(s, a)$ holds, we say that the action a is enabled by K in s .

The set of states $\{s \in S \mid \exists a \ K(s, a)\}$ for which at least an action is enabled is denoted by $\text{dom}(K)$.

$\mathcal{S}^{(K)}$ denotes the closed loop system, that is the LTS $(S, \mathcal{A}, T^{(K)})$, where $T^{(K)}(s, a, s') = T(s, a, s') \wedge K(s, a)$.

We call a path π *fullpath* if either it is infinite or its last state $\pi^{(S)}(|\pi|)$ has no successors (i.e. $\text{Adm}(\mathcal{S}, \pi^{(S)}(|\pi|)) = \emptyset$). $\text{Path}(s, a)$ denotes the set of fullpaths starting in state s with action a , i.e. the set of fullpaths π s.t. $\pi^{(S)}(0) = s$ and $\pi^{(A)}(0) = a$. Given a path π in \mathcal{S} , we define $j(\mathcal{S}, \pi, G)$ as follows. If there exists $n > 0$ s.t. $\pi^{(S)}(n) \in G$, then $j(\mathcal{S}, \pi, G) = \min\{n \mid n > 0 \wedge \pi^{(S)}(n) \in G\}$. Otherwise, $j(\mathcal{S}, \pi, G) = +\infty$. We require $n > 0$ since our systems are nonterminating and each controllable state (including a goal state) must have a path of positive length to a goal state. Taking $\sup \emptyset = +\infty$, the *worst case distance* of a state s from the goal region G is $J(\mathcal{S}, G, s) = \sup\{j(\mathcal{S}, G, \pi) \mid \pi \in \text{Path}(s, a), a \in \text{Adm}(\mathcal{S}, s)\}$.

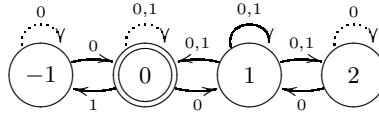


Fig. 2. The LTS \mathcal{S}_1 in Example 1.

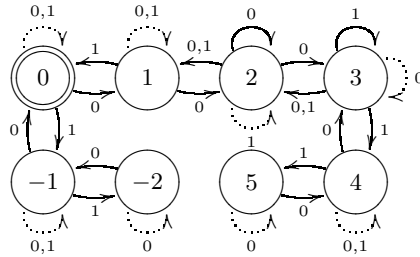


Fig. 3. The LTS \mathcal{S}_2 in Example 1.

Definition 2. An LTS control problem is a triple $\mathcal{P} = (\mathcal{S}, I, G)$. A strong solution (or simply a solution) to \mathcal{P} is a controller K for \mathcal{S} , such that $I \subseteq \text{dom}(K)$ and for all $s \in \text{dom}(K)$, $J(\mathcal{S}^{(K)}, G, s)$ is finite.

A solution K^* to \mathcal{P} is optimal if for all solutions K to \mathcal{P} , for all $s \in S$, we have $J(\mathcal{S}^{(K^*)}, G, s) \leq J(\mathcal{S}^{(K)}, G, s)$.

Example 1. Let $\mathcal{S}_1 = (S_1, \mathcal{A}_1, T_1)$ be the LTS in Fig. 2 and let $\mathcal{S}_2 = (S_2, \mathcal{A}_2, T_2)$ be the LTS in Fig. 3. S_1 is the integer interval $[-1, 2]$ and $S_2 = [-2, 5]$. $\mathcal{A}_1 = \mathcal{A}_2 = \{0, 1\}$ and the transition relations T_1 and T_2 are defined by all solid arrows in the pictures. Let $I_1 = S_1$, $I_2 = S_2$ and let $G = \{0\}$. There is no solution to the control problem (\mathcal{S}_1, I_1, G) . Because of the self-loops of the state 1, we have that both $j(\mathcal{S}_1, G, 1, 0) = +\infty$ and $j(\mathcal{S}_1, G, 1, 1) = +\infty$. The controller K_2 defined by $K_2(s, a) \equiv ((s = 1 \vee s =$

$2) \wedge a = 1) \vee (s \neq 1 \wedge s \neq 2 \wedge a = 0)$ is an optimal strong solution for the control problem (\mathcal{S}_2, I_2, G) .

2.4 Discrete Time Linear Hybrid Systems

In this section we introduce the class of discrete time Hybrid Systems that we use as plant models, namely *Discrete Time Linear Hybrid Systems* (DTLHSs for short).

Definition 3. A Discrete Time Linear Hybrid System is a tuple $\mathcal{H} = (X, U, Y, N)$ where:

- $X = X^r \cup X^d$ is a finite sequence of real (X^r) and discrete (X^d) present state variables. We denote with X' the sequence of next state variables obtained by decorating with ' all variables in X .
- $U = U^r \cup U^d$ is a finite sequence of input variables.
- $Y = Y^r \cup Y^d$ is a finite sequence of auxiliary variables that are typically used to model modes (e.g., from switching elements such as diodes) or “local” variables.
- $N(X, U, Y, X')$ is a guarded predicate over $X \cup U \cup Y \cup X'$ defining the transition relation (next state).

The semantics of DTLHSs is given in terms of LTSs.

Definition 4. Let $\mathcal{H} = (X, U, Y, N)$ be a DTLHS. The dynamics of \mathcal{H} is defined by the Labeled Transition System $\text{LTS}(\mathcal{H}) = (\mathcal{D}_X, \mathcal{D}_U, \tilde{N})$ where: $\tilde{N} : \mathcal{D}_X \times \mathcal{D}_U \times \mathcal{D}_X \rightarrow \mathbb{B}$ is a function s.t. $\tilde{N}(x, u, x') \equiv \exists y \in \mathcal{D}_Y N(x, u, y, x')$. A state x for \mathcal{H} is a state x for $\text{LTS}(\mathcal{H})$ and a run (or path) for \mathcal{H} is a run for $\text{LTS}(\mathcal{H})$ (Sect. 2.2).

2.5 DTLHS Control Problem

A DTLHS control problem (\mathcal{H}, I, G) is defined as the LTS control problem $(\text{LTS}(\mathcal{H}), I, G)$. To accommodate quantization errors, always present in software based controllers, it is useful to relax the notion of solution by tolerating an arbitrarily small error ε on the continuous variables.

Let $\varepsilon > 0$ be a real number, $W \subseteq \mathbb{R}^n \times \mathbb{Z}^m$. The ε -relaxation of W is the ball of radius ε $\mathcal{B}_\varepsilon(W) = \{(z_1, \dots, z_n, q_1, \dots, q_m) \mid \exists (x_1, \dots, x_n, q_1, \dots, q_m) \in W \text{ and } \forall i \in [n] |z_i - x_i| \leq \varepsilon\}$.

Definition 5. Let (\mathcal{H}, I, G) be a DTLHS control problem and ε be a nonnegative real number. An ε solution to (\mathcal{H}, I, G) is a solution to the LTS control problem $(\text{LTS}(\mathcal{H}), I, \mathcal{B}_\varepsilon(G))$.

Example 2. Let T be the positive constant $1/10$ (sampling time). We define the DTLHS $\mathcal{H} = (\{x\}, \{u\}, \emptyset, N)$ where x is a continuous variable, u is boolean, and $N(x, u, x') \equiv [\bar{u} \rightarrow x' = x + (5/4 - x)T] \wedge [u \rightarrow x' = x + (x - 7/4)T]$. Let $I(x) \equiv -1 \leq x \leq 5/2$ and $G(x) \equiv x = 0$. Finally, let \mathcal{P} be the control problem (\mathcal{H}, I, G) . A controller may drive the system near to the goal G , by enabling a suitable action in such a way that $x' < x$ when $x > 0$ and $x' > x$ when $x < 0$. However the controller $K(x, u)$

defined by $K(x, u) \equiv (-1 \leq x < 0 \wedge \bar{u}) \vee (0 \leq x < 2 \wedge u) \vee (1 \leq x \leq 5/2 \wedge \bar{u})$ is not a solution, because it allows infinite paths to be executed. Since $K(5/4, 0)$ and $N(5/4, 0, 5/4)$ hold, the closed loop system $\mathcal{H}^{(K)}$ may loop forever along the path $5/4, 0, 5/4, 0 \dots$. K' defined by $K'(x, u) \equiv (-1 \leq x < 0 \wedge \bar{u}) \vee (0 \leq x \leq 3/2 \wedge u) \vee (3/2 \leq x \leq 5/2 \wedge \bar{u})$ is a solution to \mathcal{P} .

2.6 Quantized Control Problem

As usual in classical control theory, *quantization* (e.g., see [20]) is the process of approximating a continuous interval by a set of integer values. In the following we formally define the quantized feedback control problem for DTLHSs.

A *quantization function* γ for a real interval $I = [a, b]$ is a non-decreasing function $\gamma : I \mapsto \mathbb{Z}$ s.t. $\gamma(I)$ is a bounded integer interval. We will denote $\gamma(I)$ as $\hat{I} = [\gamma(a), \gamma(b)]$. The *quantization step* of γ , notation $\|\gamma\|$, is defined as $\sup\{|w - z| \mid w, z \in I \wedge \gamma(w) = \gamma(z)\}$. For ease of notation, we extend quantizations to integer intervals, by stipulating that in such a case the quantization function is the identity function.

Definition 6. Let $\mathcal{H} = (X, U, Y, N)$ be a DTLHS, and $W = X \cup U \cup Y$. A quantization \mathcal{Q} for \mathcal{H} is a pair (A, Γ) , where:

- A is a predicate over W that explicitly bounds each variable in W (i.e., $A = \bigwedge_{w \in W} \alpha_w \leq w \leq \beta_w$, with $\alpha_w, \beta_w \in \mathcal{D}_W$). For each $w \in W$, we denote with $A_w = [\alpha_w, \beta_w]$ its admissible region and with $A_W = \prod_{w \in W} A_w$.
- Γ is a set of maps $\Gamma = \{\gamma_w \mid w \in W \text{ and } \gamma_w \text{ is a quantization function for } A_w\}$.

Let $W = [w_1, \dots, w_k]$ and $v = [v_1, \dots, v_k] \in A_W$. We write $\Gamma(v)$ for the tuple $[\gamma_{w_1}(v_1), \dots, \gamma_{w_k}(v_k)]$. Finally, the quantization step $\|\Gamma\|$ is defined as $\sup\{\|\gamma\| \mid \gamma \in \Gamma\}$.

A control problem admits a *quantized solution* if control decisions can be made by just looking at quantized values. This enables a software implementation for a controller.

Definition 7. Let $\mathcal{H} = (X, U, Y, N)$ be a DTLHS, $\mathcal{Q} = (A, \Gamma)$ be a quantization for \mathcal{H} and $\mathcal{P} = (\mathcal{H}, I, G)$ be a DTLHS control problem. A \mathcal{Q} Quantized Feedback Control (QFC) solution to \mathcal{P} is a $\|\Gamma\|$ solution $K(x, u)$ to \mathcal{P} such that $K(x, u) = \hat{K}(\Gamma(x), \Gamma(u))$ where $\hat{K} : \Gamma(A_X) \times \Gamma(A_U) \rightarrow \mathbb{B}$.

Example 3. Let \mathcal{P} , K and K' be as in Ex. 2. Let us consider the quantizations $\mathcal{Q}_1 = (A_1, \Gamma_1)$, where $A_1 = I$, $\Gamma_1 = \{\gamma_x\}$ and $\gamma_x(x) = \lfloor x \rfloor$. The set $\Gamma(A_x)$ of quantized states is the integer interval $[-1, 2]$. No \mathcal{Q} QFC solution can exist, because in state 1 either enabling action 1 or action 0 allows infinite loops to be potentially executed in the closed loop system. The controller K' in Ex. 2 can be obtained as a quantized controller decreasing the quantization step, for example, by considering the quantization $\mathcal{Q}_2 = (A_2, \Gamma_2)$, where $A_2 = A_1$, $\Gamma_2 = \{\tilde{\gamma}_x\}$ and $\tilde{\gamma}_x(x) = \lfloor 2x \rfloor$.

3 Control Abstraction Computation

As explained in Sect. 1.1, the heaviest computation step for *QKS* is the computation of the control abstraction. In this section, we recall the definition of control abstraction, as well as how it is computed by *QKS*.

In the following, let $\mathcal{H} = (X, U, Y, N)$ and $\mathcal{Q} = (A, \Gamma)$ be, respectively, a DTLHS and a quantization for \mathcal{H} . We say that an action $\hat{u} \in \Gamma(A_U)$ is \mathcal{Q} -admissible in a state $\hat{x} \in \Gamma(A_X)$ iff, for all plant states $x \in \Gamma^{-1}(\hat{x})$ and plant actions $u \in \Gamma^{-1}(\hat{u})$, and for all plant states x' s.t. (x, u, x') is a transition in $\text{LTS}(\mathcal{H})$, we have that $x' \in A_X$ (that is, \hat{u} always maintain the plant inside its admissible region when starting from \hat{x}). Given this, a \mathcal{Q} control abstraction is an LTS $\hat{\mathcal{H}} = (\Gamma(A_X), \Gamma(A_U), \hat{N})$, where for \hat{N} the following holds: i) each abstract transition in \hat{N} stems from a concrete transition in N ; ii) each concrete transition in N is faithfully represented by an abstract transition in \hat{N} , whenever it is not a self loop and its corresponding abstract action is \mathcal{Q} -admissible; iii) if there is no upper bound to the length of concrete paths in $\text{LTS}(\mathcal{H})$ which are all inside the counter-image of an abstract state then there is an abstract self loop in \hat{N} .

We are now ready to give details about control abstraction generation. Namely, function *minCtrAbs* in Alg. 1, given a quantization $\mathcal{Q} = (A, \Gamma)$ for a DTLHS $\mathcal{H} = (X, U, Y, N)$, computes a \mathcal{Q} -control abstraction $(\Gamma(A_X), \Gamma(A_U), \hat{N})$ of \mathcal{H} . Namely, for each abstract state \hat{x} (line 2) an auxiliary function *minCtrAbsAux* is called. On its side, function *minCtrAbsAux* decides which transitions, among all the possible ones starting from \hat{x} , fulfills the definition of control abstraction given above, and thus may be inserted in \hat{N} . The checks in lines 2, 3 and 6, and the computation in line 4, are performed by properly defining MILP problems, which are solved using known algorithms (available in the GLPK package).

Algorithm 1 Building control abstractions

Input: DTLHS $\mathcal{H} = (X, U, Y, N)$, quantization $\mathcal{Q} = (A, \Gamma)$.

function *minCtrAbs* (\mathcal{H}, \mathcal{Q})

1. $\hat{N} \leftarrow \emptyset$
 2. **for all** $\hat{x} \in \Gamma(A_X)$ **do**
 3. $\hat{N} \leftarrow \text{minCtrAbsAux}(\mathcal{H}, \mathcal{Q}, \hat{x}, \hat{N})$
 4. **return** $(\Gamma(A_X), \Gamma(A_U), \hat{N})$
-

4 Parallel Synthesis of Control Software

In this section we present our novel parallel algorithm for the control abstraction generation of a given DTLHS. Such algorithm is a parallel version (for distributed memory systems such as computer clusters) of the standalone Alg. 1. In this way, i.e. by improving the performance on the bottleneck of *QKS*, we obtain a significant speedup for the whole approach to the synthesis of control software for DTLHSs.

Algorithm 2 Building control abstractions: auxiliary function

Input: DTLHS \mathcal{H} , quantization \mathcal{Q} , abstract state \hat{x} , partial control abstraction \hat{N} .

function $\text{minCtrAbsAux}(\mathcal{H}, \mathcal{Q}, \hat{x}, \hat{N})$

1. **for all** $\hat{u} \in \Gamma(A_U)$ **do**
 2. **if** $\neg \mathcal{Q}\text{-admissible}(\mathcal{H}, \mathcal{Q}, \hat{x}, \hat{u})$ **then continue**
 3. **if** $\text{selfLoop}(\mathcal{H}, \mathcal{Q}, \hat{x}, \hat{u})$ **then** $\hat{N} \leftarrow \hat{N} \cup \{(\hat{x}, \hat{u}, \hat{x})\}$
 4. $\mathcal{O} \leftarrow \text{overImg}(\mathcal{H}, \mathcal{Q}, \hat{x}, \hat{u})$
 5. **for all** $\hat{x}' \in \Gamma(\mathcal{O})$ **do**
 6. **if** $\hat{x} \neq \hat{x}' \wedge \text{existsTrans}(\mathcal{H}, \mathcal{Q}, \hat{x}, \hat{u}, \hat{x}')$ **then**
 7. $\hat{N} \leftarrow \hat{N} \cup \{(\hat{x}, \hat{u}, \hat{x}')\}$
 8. **return** \hat{N}
-

In the following, let $\mathcal{H} = (X, U, Y, N)$ and $\mathcal{Q} = (A, \Gamma)$ be, respectively, the DTLHS and the quantization in input to our algorithm for control abstraction generation. Moreover, let p be the number of available processors (cores) in the cluster of multicore processors.

Our parallel algorithm rests on observing that, for each abstract state $\hat{x} \in \Gamma(A_X)$, all statements in the **for** loop of lines 2–7 of Alg. 1 are carried out independently of the computations needed for any other abstract state $\hat{\xi}$. This observation allows us to use known techniques targeting *embarrassingly parallel* problems to obtain a significant speedup on the control abstraction generation phase.

To this aim, we use a map-reduce based parallelization technique. Namely, a *master* node of a computer cluster assigns (*map*) the computations needed for an abstract state \hat{x} (i.e., lines 1–7 of Alg. 1) to one of n available nodes (*workers*), so that each worker approximately handles $\frac{|\Gamma(A_X)|}{n}$ abstract states, thus balancing the parallel workload. Once a worker has completed the computations needed for all its abstract states, thus obtaining a local control abstraction, it sends back to the master such local control abstraction. The master node collects the local control abstractions and compose them (with a logical OR operation) in order to obtain the desired global control abstraction. Note that, as in *embarrassingly parallel* tasks, communication only takes place at the beginning and at the end of local computations.

More in detail, as for the mapping phase, our parallel algorithm rests on partitioning the (finite) abstract state space $\Gamma(A_X)$ into p subspaces $\Gamma^{(1,p)}(A_X), \dots, \Gamma^{(p,p)}(A_X)$, thus $\Gamma^{(i,p)}(A_X) \cap \Gamma^{(j,p)}(A_X) = \emptyset$ for $i \neq j$ and $\cup_{i=0}^{p-1} \Gamma^{(i,p)}(A_X) = \Gamma(A_X)$. We design such a partition so that we can locally check if $\hat{x} \in \Gamma^{(i,p)}(A_X)$, i.e. processor i may check this by only knowing i, p and \hat{x} . This allows us to avoid sending to each worker the explicit list of abstract states it has to work on, since it suffices to simply send i and p (together with the overall input \mathcal{H} and \mathcal{Q}) to the worker i . To this aim, let $\text{ord}: \Gamma(A_X) \rightarrow [|\Gamma(A_X)|]$ be s.t. $\text{ord}(\hat{x}) = m$ iff \hat{x} is the m -th abstract state in the lexicographical ordering of $\Gamma(A_X)$. Then, $\Gamma^{(i,p)}(A_X) = \{\hat{x} \in \Gamma(A_X) \mid ((\text{ord}(\hat{x}) - 1) \bmod p) + 1 = i\}$, being \bmod the modulus operation. For an example, see the “MAP” arrow in Fig. 4.

We outline our novel parallel algorithm in Algs. 4 (for worker nodes) and 3 (for the master node). An example of an execution is given in Fig. 4. Note that the master node will need to know the number p of available workers (line 4 of Alg. 3), while workers

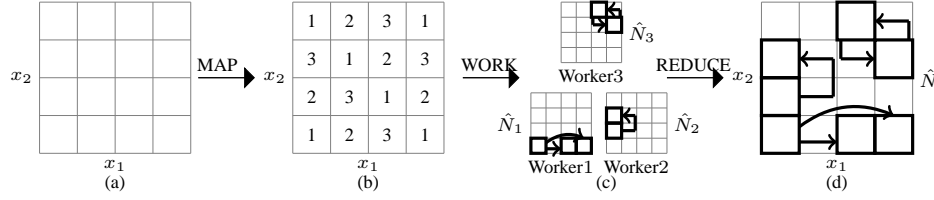


Fig. 4. Example of execution of the parallel algorithm (see Ex. 4).

also knows their index i (line 4 of Alg. 4), which is sent by the master itself. Alg. 4 is similar to Alg. 1, except that only abstract states $\hat{x} \in \Gamma^{(i,p)}(A_X)$ are considered in line 2, and that a local control abstraction \hat{N}_i (represented by an OBDD [21]) is computed. This entails that the global control abstraction \hat{N} has to be computed (lines 3–4 of Alg. 3) once all workers have finished their local computation.

Example 4. Let $\mathcal{H} = (X, U, Y, N)$ be a DTLHS and \mathcal{Q} a quantization for \mathcal{H} s.t. $X = [x_1, x_2]$ and \mathcal{Q} discretizes both x_1, x_2 with two bits. E.g., this may be the case if $x_1 \in [4]$ is a discrete variable, thus needing two bits for quantization, and x_2 is quantized with two bits. Thus, the starting status for function *minCtrAbsMaster* in Alg. 3 with input parameters \mathcal{H} , \mathcal{Q} and 3 (number of workers) is the one depicted in Fig. 4.a, where each cell corresponds to an abstract state. Then, function *minCtrAbsMaster* maps the workload among the 3 workers as it is shown in Fig. 4.b, where abstract states labeled with $i \in [3]$ will be handled by worker i . Fig. 4.c shows how each worker i computes its local control abstraction \hat{N}_i , under the assumption each local control abstraction only has the shown transitions. Finally, Fig. 4.d shows how the master rejoins the local abstractions in order to get the final one, i.e. \hat{N} .

Algorithm 3 Building control abstractions in parallel: master node

Input: DTLHS \mathcal{H} , quantization \mathcal{Q} , workers number p

function *minCtrAbsMaster* (\mathcal{H} , \mathcal{Q} , p)

1. **for all** $i \in \{1, \dots, p\}$ **do**
 2. create a worker and send \mathcal{H} , \mathcal{Q} , i and p to it /* map step */
 3. wait to get $\hat{N}_1, \dots, \hat{N}_p$ from workers /* reduce step */
 4. **return** $(\Gamma(A_X), \Gamma(A_U), \cup_{j=1}^p \hat{N}_j)$
-

4.1 Implementation with MPI

We actually implemented Algs. 4 and 3 in *PQKS* by using MPI (Message Passing Interface, see [22]). Since MPI is widely used, this allows us to run *PQKS* on nearly all computer clusters. Note that in MPI all nodes (processors) execute the same program (SPMD paradigm), each one knowing its rank i and the number of processors p . Thus

Algorithm 4 Building control abstractions in parallel: worker node

Input: DTLHS $\mathcal{H} = (X, U, Y, N)$, quantization $\mathcal{Q} = (A, I)$, index i , workers number p

function *parMinCtrAbs* ($\mathcal{H}, \mathcal{Q}, i, p$)

1. $\hat{N}_i \leftarrow \emptyset$
 2. **for all** $\hat{x} \in \Gamma^{(i,p)}(A_X)$ **do**
 3. $\hat{N}_i \leftarrow \text{minCtrAbsAux}(\mathcal{H}, \mathcal{Q}, \hat{x}, \hat{N}_i)$
 4. send \hat{N}_i to the master
-

lines 1–2 of Alg. 3 are directly implemented by the MPI framework. Finally, in our implementation the master node is not a separate node, but it actually performs like a worker while waiting for local control abstractions from (other) workers. Local control abstraction from other workers are collected once the master local control abstraction has been performed. This allows us to use p nodes instead of $p + 1$.

Note that lines 4 and 3 of, respectively, Algs. 4 and 3 require workers to send their local control abstraction to the master. Being control abstractions represented as OBDDs, which are sparse data structures, this step may be difficult to be implemented with the a call to `MPI_Send` (as it is usually done in MPI programs), which is designed for contiguous data. In our experiments, workers use known algorithms (implemented in the CUDD package) to efficiently dump the OBDD representing their local control abstraction on the shared filesystem and then performs an `MPI_Barrier` call in order to synchronize all workers with the master. After this, the master node collects local control abstraction from workers, by reloading them from the shared filesystem, in order to build the final global one. Consequently, when presenting experimental results in Sect. 5, we include I/O time in communication time. Note that communication based on shared filesystem is very common also in MapReduce native implementations like Hadoop [5].

Finally, Algs. 4 and 3 may conceptually be implemented on multithreaded systems with shared memory. However, in our implementation we use GLPK as external library to solve MILP problems required in computations inside function *minCtrAbsAux* (see Alg. 2). Since GLPK is not thread-safe, we may not implement Algs. 3 and 4 on multithreaded shared memory systems.

5 Experimental Results

In this section we present experimental results obtained by using our parallel approach on two meaningful and challenging examples for the automatic synthesis of correct-by-construction control software, namely the inverted pendulum and multi-input buck DC-DC converter. To this aim, we show the gain of the parallel approach with respect to the serial algorithm, also providing standard measures such as communication and I/O time.

We implement functions *minCtrAbsMaster* and *parMinCtrAbs* of Algs. 3 and 4 in C programming language using the CUDD package for OBDD based computations and the GLPK package for MILP problems solving, and MPI for the parallel setting and communication. The resulting tool, *PQKS* (*Parallel QKS*), extends the tool *QKS* [2]

by replacing function *minCtrAbs* of Alg. 1 with function *minCtrAbsMaster* of Alg. 3. We run *PQKS* for different number of bits of AD conversion and increasing number of processors involved.

In Sect. 5.1 and 5.2 we will present the DTLHS models of the inverted pendulum and the multi-input buck DC-DC converter, on which our experiments focus. In Sect. 5.3 we give the details of the experimental setting, and finally, in Sect. 5.4, we discuss experimental results.

5.1 The Inverted Pendulum as a DTLHS

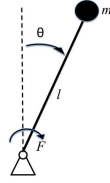


Fig. 5. Inverted Pendulum with Stationary Pivot Point.

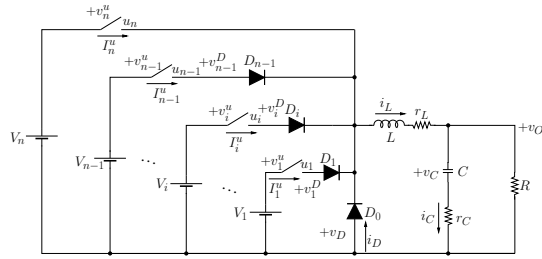


Fig. 6. Multi-input Buck DC-DC converter.

The inverted pendulum [7] (see Fig. 5) is modeled by taking the angle θ and the angular velocity $\dot{\theta}$ as state variables. The input of the system is the torquing force $u \cdot F$, that can influence the velocity in both directions. Here, the variable u models the direction and the constant F models the intensity of the force. Differently from [7], we consider the problem of finding a discrete controller, whose decisions may be only “apply the force clockwise” ($u = 1$), “apply the force counterclockwise” ($u = -1$), or “do nothing” ($u = 0$). The behaviour of the system depends on the pendulum mass m , the length of the pendulum l , and the gravitational acceleration g . Given such parameters, the motion of the system is described by the differential equation $\ddot{\theta} = \frac{g}{l} \sin \theta + \frac{1}{ml^2} uF$. In order to obtain a state space representation, we consider the following normalized system, where x_1 is the angle θ and x_2 is the angular speed $\dot{\theta}$:

$$\begin{cases} \dot{x}_1 = x_2 \\ \dot{x}_2 = \frac{g}{l} \sin x_1 + \frac{1}{ml^2} uF \end{cases} \quad (1)$$

The discrete time model obtained from the equations in (1) by introducing a constant T that models the sampling time is:

$$(x'_1 = x_1 + Tx_2) \wedge (x'_2 = x_2 + T\frac{g}{l} \sin x_1 + T\frac{1}{ml^2} uF)$$

that is not linear, as it contains the function $\sin x_1$. A linear model can be found by under- and over-approximating the non linear function $\sin x$. In our experiments, we will consider the linear model obtained as follows.

First of all, in order to exploit sinus periodicity, we consider the equation $x_1 = 2\pi y_k + y_\alpha$, where y_k represents the period in which x_1 lies and $y_\alpha \in [-\pi, \pi]^3$ represents the actual x_1 inside a given period. Then, we partition the interval $[-\pi, \pi]$ in four intervals: $I_1 = [-\pi, -\frac{\pi}{2}]$, $I_2 = [-\frac{\pi}{2}, 0]$, $I_3 = [0, \frac{\pi}{2}]$, $I_4 = [\frac{\pi}{2}, \pi]$. In each interval I_i ($i \in [4]$), we consider two linear functions $f_i^+(x)$ and $f_i^-(x)$, such that for all $x \in I_i$, we have that $f_i^-(x) \leq \sin x \leq f_i^+(x)$. As an example, $f_1^+(y_\alpha) = -0.637y_\alpha - 2$ and $f_1^-(y_\alpha) = -0.707y_\alpha - 2.373$.

Let us consider the set of fresh continuous variables $Y^r = \{y_\alpha, y_{\sin}\}$ and the set of fresh discrete variables $Y^d = \{y_k, y_q, y_1, y_2, y_3, y_4\}$, being y_1, \dots, y_4 boolean variables. The DTLHS model \mathcal{I}_F for the inverted pendulum is the tuple (X, U, Y, N) , where $X = \{x_1, x_2\}$ is the set of continuous state variables, $U = \{u\}$ is the set of input variables, $Y = Y^r \cup Y^d$ is the set of auxiliary variables, and the transition relation $N(X, U, Y, X')$ is the following predicate:

$$\begin{aligned} & (x'_1 = x_1 + 2\pi y_q + T x_2) \wedge (x'_2 = x_2 + T \frac{g}{l} y_{\sin} + T \frac{1}{ml^2} u F) \\ & \wedge \bigwedge_{i \in [4]} y_i \rightarrow f_i^-(y_\alpha) \leq y_{\sin} \leq f_i^+(y_\alpha) \\ & \wedge \bigwedge_{i \in [4]} y_i \rightarrow y_\alpha \in I_i \wedge \sum_{i \in [4]} y_i \geq 1 \\ & \wedge x_1 = 2\pi y_k + y_\alpha \wedge -\pi \leq x'_1 \leq \pi \end{aligned}$$

Overapproximations of the system behaviour increase system nondeterminism. Since \mathcal{I}_F dynamics overapproximates the dynamics of the non-linear model, the controllers that we synthesize are inherently *robust*, that is they meet the given closed loop requirements *notwithstanding* nondeterministic small *disturbances* such as variations in the plant parameters. Tighter overapproximations of non-linear functions makes finding a controller easier, whereas coarser overapproximations makes controllers more robust.

The typical goal for the inverted pendulum is to turn the pendulum steady to the up-right position, starting from any possible initial position, within a given speed interval.

5.2 Multi-input Buck DC-DC Converter

The *multi-input* buck DC-DC converter [6] in Fig. 6 is a mixed-mode analog circuit converting the DC input voltage (V_i in Fig. 6) to a desired DC output voltage (v_O in Fig. 6). As an example, buck DC-DC converters are used off-chip to scale down the typical laptop battery voltage (12-24) to the just few volts needed by the laptop processor (e.g. [23]) as well as on-chip to support *Dynamic Voltage and Frequency Scaling* (DVFS) in multicore processors (e.g. [24]). Because of its widespread use, control schemas for buck DC-DC converters have been widely studied (e.g. see [24,23]). The typical software based approach (e.g. see [23]) is to control the switches u_1, \dots, u_n in Fig. 6 (typically implemented with a MOSFET) with a microcontroller.

In such a converter (Fig. 6), there are n power supplies with voltage values V_1, \dots, V_n , n switches with voltage values v_1^u, \dots, v_n^u and current values I_1^u, \dots, I_n^u , and n input diodes D_0, \dots, D_{n-1} with voltage values v_0^D, \dots, v_{n-1}^D and current i_0^D, \dots, i_{n-1}^D (in the following, we will write v_D for v_0^D and i_D for i_0^D).

³ In this section we write π for a rational approximation of it.

The circuit state variables are i_L and v_C . However we can also use the pair i_L, v_O as state variables in the DTLHS model since there is a linear relationship between i_L, v_C and v_O , namely: $v_O = \frac{r_C R}{r_C + R} i_L + \frac{R}{r_C + R} v_C$. We model the n -input buck DC-DC converter with the DTLHS $\mathcal{B}_n = (X, U, Y, N)$, with $X = [i_L, v_O]$, $U = [u_1, \dots, u_n]$, $Y = [v_D, v_1^D, \dots, v_{n-1}^D, i_D, I_1^u, \dots, I_n^u, v_1^u, \dots, v_n^u]$.

The transition relation N is as follows. From a simple circuit analysis (e.g. see [25]) we have the following equations:

$$\dot{i}_L = a_{1,1} i_L + a_{1,2} v_O + a_{1,3} v_D$$

$$\dot{v}_O = a_{2,1} i_L + a_{2,2} v_O + a_{2,3} v_D$$

where the coefficients $a_{i,j}$ depend on the circuit parameters R, r_L, r_C, L and C in the following way: $a_{1,1} = -\frac{r_L}{L}$, $a_{1,2} = -\frac{1}{L}$, $a_{1,3} = -\frac{1}{L}$, $a_{2,1} = \frac{R}{r_C + R} [-\frac{r_C r_L}{L} + \frac{1}{C}]$, $a_{2,2} = \frac{-1}{r_C + R} [\frac{r_C R}{L} + \frac{1}{C}]$, $a_{2,3} = -\frac{1}{L} \frac{r_C R}{r_C + R}$. Using a discrete time model with sampling time T (writing x' for $x(t+1)$) we have:

$$i'_L = (1 + T a_{1,1}) i_L + T a_{1,2} v_O + T a_{1,3} v_D$$

$$v'_O = T a_{2,1} i_L + (1 + T a_{2,2}) v_O + T a_{2,3} v_D.$$

The algebraic constraints stemming from the constitutive equations of the switching elements are the following:

$$\begin{array}{ll} q_0 \rightarrow v_D = R_{\text{on}} i_D & \bar{q}_0 \rightarrow v_D = R_{\text{off}} i_D \\ q_0 \rightarrow i_D \geq 0 & \bar{q}_0 \rightarrow v_D \leq 0 \\ \bigwedge_{i=1}^{n-1} q_i \rightarrow v_i^D = R_{\text{on}} I_i^u & \bigwedge_{i=1}^{n-1} \bar{q}_i \rightarrow v_i^D = R_{\text{off}} I_i^u \\ \bigwedge_{i=1}^{n-1} q_i \rightarrow I_i^u \geq 0 & \bigwedge_{i=1}^{n-1} \bar{q}_i \rightarrow v_i^D \leq 0 \\ \bigwedge_{j=1}^n u_j \rightarrow v_j^u = R_{\text{on}} I_j^u & \bigwedge_{j=1}^n \bar{u}_j \rightarrow v_j^u = R_{\text{off}} I_j^u \\ i_L = i_D + \sum_{i=1}^n I_i^u & v_D = v_i^u + v_i^D - V_i \\ & v_D = v_n^u - V_n \end{array}$$

The typical goal for a multi-input buck is to drive i_L and v_O within given goal intervals.

5.3 Experimental Setting

All experiments have been carried out on a cluster with 4 nodes and Open MPI implementation of MPI. Each node contains 4 quad-core 2.83 GHz Intel Xeon E5440 processors. Nodes share common filesystem. We have run maximum 15 processors per node.

In the inverted pendulum \mathcal{I}_F with force intensity F , as in [7], we set pendulum parameters l and m in such a way that $\frac{g}{l} = 1$ (i.e. $l = g$) $\frac{1}{ml^2} = 1$ (i.e. $m = \frac{1}{l^2}$). As for the quantization, we set $A_{x_1} = [-1.1\pi, 1.1\pi]$ and $A_{x_2} = [-4, 4]$, and we define $A_{\mathcal{I}_F} = A_{x_1} \times A_{x_2} \times A_u$.

In the multi-input buck DC-DC converter with n inputs \mathcal{B}_n , we set constant parameters as follows: $L = 2 \cdot 10^{-4}$ H, $r_L = 0.1 \Omega$, $r_C = 0.1 \Omega$, $R = 5 \Omega$, $C = 5 \cdot 10^{-5}$ F, $R_{\text{on}} = 0 \Omega$, $R_{\text{off}} = 10^4 \Omega$, and $V_i = 10i$ V for $i \in [n]$. As for the quantization, we set $A_{i_L} = [-4, 4]$ and $A_{v_O} = [-1, 7]$, and we define $A_{\mathcal{B}_n} = A_{i_L} \times A_{v_O} \times A_{u_1} \times \dots \times A_{u_n}$.

In both examples, we use uniform quantization functions dividing the domain of each state variable x into 2^b equal intervals, where b is the number of bits used by AD conversion. The resulting quantizations are $\mathcal{Q}_{\mathcal{I}_F, b} = (A_{\mathcal{I}_F}, \Gamma_b)$ and $\mathcal{Q}_{\mathcal{B}_n, b} = (A_{\mathcal{B}_n}, \Gamma_b)$. Since both examples have two quantized variables, each one with b bits, the number of quantized (abstract) states is exactly 2^{2b} .

We run *QKS* and *PQKS* on the inverted pendulum model \mathcal{I}_F with $F = 0.5N$ (force intensity), and on the multi-input buck DC-DC model \mathcal{B}_n , with $n = 5$ (number of inputs). For the inverted pendulum, we use sampling time $T = 0.01$ seconds. For the multi-input buck, we set $T = 10^{-6}$ seconds. For both systems, we run experiments varying the number of bits $b = 9, 10$ (also 11 for the inverted pendulum) and the number of processors (workers) $p = 1, 10, 20, 30, 40, 50, 60$. Finally, we show how *PQKS* is useful when applied to examples requiring a huge computation time by considering the inverted pendulum with $b = 13$, where control abstraction is computed with $p = 1$ and $p = 60$.

Table 1. Experimental Results for inverted pendulum.

b	QKS	PQKS					CPU K
	CPU Ctrabs	p CPU Ctrabs	CT	IO	Speedup	Efficiency	
9	8.958e+03	50 2.064e+02	7.696e+02	1.540e+01	43.399	86.798	2.970e+01
9	8.958e+03	60 1.763e+02	6.825e+02	1.790e+01	50.809	84.681	2.970e+01
10	3.108e+04	50 8.527e+02	3.112e+03	7.330e+01	36.450	72.900	1.131e+02
10	3.108e+04	60 7.173e+02	2.170e+03	6.740e+01	43.331	72.218	1.131e+02
11	1.147e+05	50 3.504e+03	1.242e+04	2.840e+02	32.742	65.485	1.131e+03
11	1.147e+05	60 2.938e+03	6.762e+03	2.842e+02	39.050	65.084	1.131e+03

Table 2. Experimental Results for multi-input buck DC-DC converter.

b	QKS	PQKS					CPU K
	CPU Ctrabs	p CPU Ctrabs	CT	IO	Speedup	Efficiency	
9	1.300e+05	50 4.020e+03	1.582e+04	4.100e+01	32.347	64.694	7.400e+01
9	1.300e+05	60 3.363e+03	6.550e+03	4.800e+01	38.666	64.443	7.400e+01
10	5.231e+05	50 1.619e+04	6.306e+04	1.780e+02	32.307	64.613	3.780e+02
10	5.231e+05	60 1.353e+04	2.765e+04	1.910e+02	38.657	64.428	3.780e+02

In order to evaluate effectiveness of our approach, we use the following measures: speedup, efficiency, communication time (in seconds) and I/O time (in seconds). The *speedup* of our approach is represented by the serial CPU time divided by the parallel CPU time, i.e. $\text{Speedup} = \frac{\text{serial CPU}}{\text{parallel CPU}}$. To evaluate scalability of our approach we define the *scaling efficiency* (or simply *efficiency*) as the percentage ratio between speedup and number of processors p , i.e. $\text{Efficiency} = \frac{\text{speedup}}{p} \%$. In Algs. 3 and 4, the *communication time* consists in the time needed by all workers to send their local control abstraction to the master. In agreement with Sect. 4.1, the communication time is increased by the I/O time, that is the overall time spent by processors in input/output activities.

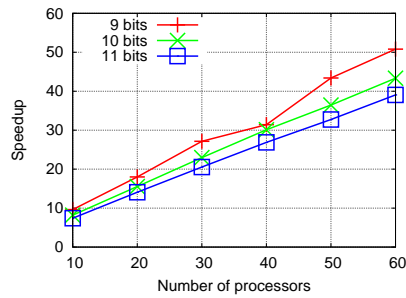


Fig. 7. Inverted pendulum: speedup.

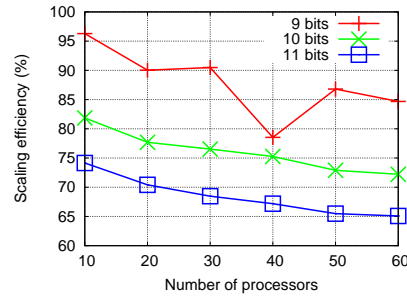


Fig. 8. Inverted pendulum: scaling efficiency.

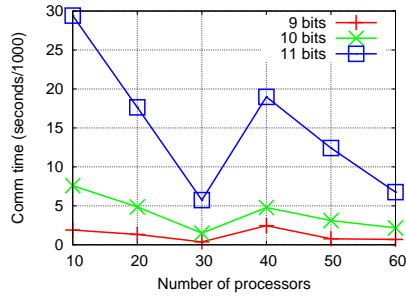


Fig. 9. Inverted pendulum: communication time.

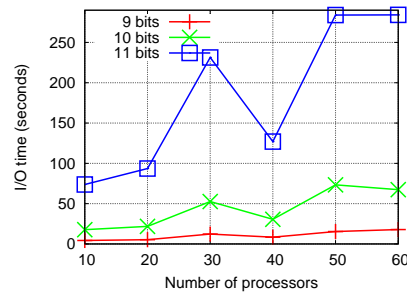


Fig. 10. Inverted pendulum: I/O time.

Figs. 7, 8, 9 and 10 show, respectively, the speedup, the scaling efficiency, the communication time (divided by 1000) and the I/O time of Algs. 3 and 4 as a function of p , for the inverted pendulum with $b = 9, 10, 11$. Analogously, Figs. 11, 12, 13 and 14

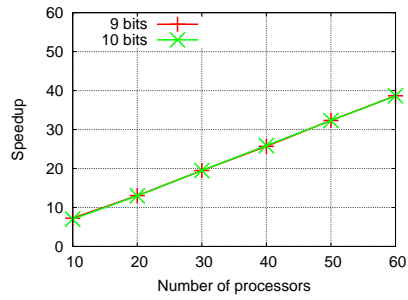


Fig. 11. Multi-input buck: speedup.

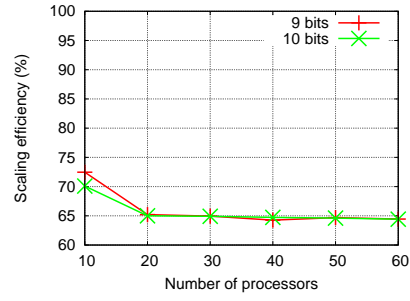


Fig. 12. Multi-input buck: scaling efficiency.

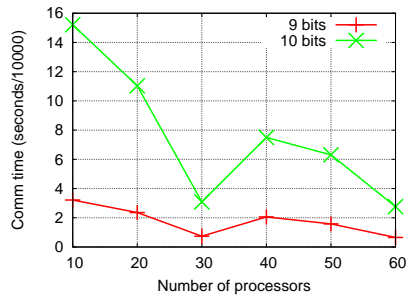


Fig. 13. Multi-input buck: communication time.

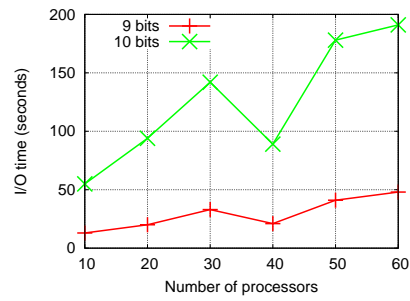


Fig. 14. Multi-input buck: I/O time.

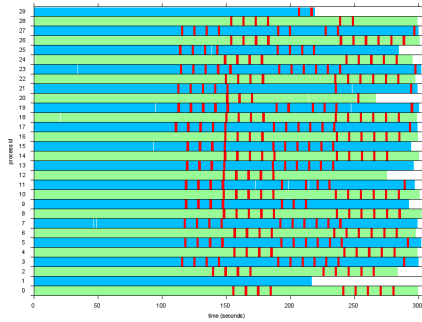


Fig. 15. Details about inverted pendulum computation time (30 nodes).

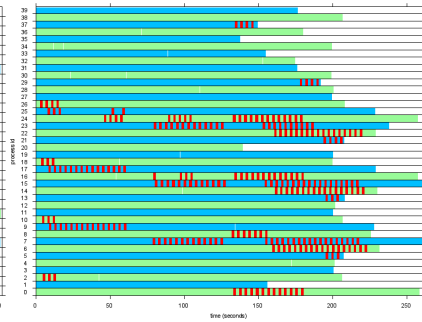


Fig. 16. Details about inverted pendulum computation time (40 nodes).

show the same measures (except for the fact that communication time is divided by 10000) for the multi-input buck with $b = 9, 10$.

We also show the absolute values for the experiments with 50 and 60 processors in Tabs. 1 and 2. Tabs. 1 and 2 have common columns. The meaning of such common columns is as follows. Column **b** is the number of bits used for quantization. Column **QKS (CPU Ctrabs)** reports the execution time in seconds needed by *QKS* to compute the control abstraction (i.e. Alg. 1). Columns **PQKS** report experimental values for *PQKS*. Namely, column p shows the number of processors, column **CPU Ctrabs** reports the execution time in seconds for Alg. 3 (i.e., the master execution time, since it wraps the overall parallel computation), column **CT** shows the communication time (including I/O time), column **IO** shows the I/O time only, column **Speedup** reports the speedup and column **Efficiency** reports the scaling efficiency. Finally, column **CPU K** shows the execution time in seconds for the control software generation (i.e., the remaining computation of *QKS*, after the control abstraction generation).

5.4 Experiments Discussion

From Figs. 7 and 11 we note that the speedup is almost linear, with a $2/3$ slope. From Figs. 8 and 12 we note that scaling efficiency remains high when increasing the number of processors p . For example, for $b = 11$ bits, our approach efficiency is in a range from 75% (10 processors) to 65% (60 processors). In any case, efficiency is always above 65%.

Figs. 9 and 13 show that communication time almost always decreases when p increases. This is motivated by the fact that, in our MPI implementation, communication among nodes takes place mostly when workers send their local control abstractions to the master via the shared filesystem. Since in our implementation this happens only after an `MPI_Barrier` (i.e., the parallel computation may proceed only when all nodes have reached an `MPI_Barrier` statement), the communication time also includes waiting time for workers which finishes their local computation before the other ones. Thus, if all workers need about the same time to complete the local computation, then the communication time is low. Note that this explains also the discontinuity when passing from 30 to 40 nodes which may be observed in the figures above. In fact, each worker has (almost) the same workload in terms of abstract states number, but some abstract states may need more computation time than others (i.e., computation time of function *minCtrAbsAux* in Alg. 2 may have significant variations on different abstract states). If such “hard” abstract states are well distributed among workers, communication time is low (with higher efficiency), otherwise it is high. Figs. 15 and 16 show such phenomenon on the inverted pendulum quantized with 9 bits, when the parallel algorithm is executed by 30 and 40 workers, respectively. In such figures, the x -axis represents computation time, the y -axis the workers, and “hard” abstract states are represented in red.

Finally, in order to show feasibility of our approach also on DTLHSs requiring a huge computation time to generate the control abstraction, we run *PQKS* on the inverted pendulum with $b = 13$. We estimate the computation time for control abstraction generation for $p = 1$ to be 25 days. On the other hand, with $p = 60$, we are able to compute the control abstraction generation in only 16 hours.

6 Conclusions and Future Work

In this paper we presented a map-reduce-style parallel algorithm (and its implementation *PQKS*) for automatic synthesis of correct-by-construction control software for discrete time linear hybrid systems, starting from a formal model of the controlled system, safety and liveness requirements and number of bits for analog-to-digital conversion. Such an algorithm significantly improves performance of an existing standalone approach (implemented in the tool *QKS*), which may require weeks or even months of computation when applied to large-size hybrid systems.

Our results show that our parallel approach on computing the control abstraction is effective. In fact, the gain obtained by *PQKS* with respect to *QKS* is shown to be very high, e.g. with 60 processors *PQKS* outputs the control software for the 13-bits quantized inverted pendulum in about 16 hours, whilst *QKS* needs about 25 days of computation.

Future work may consist in further improving the communication among processors (avoiding usage of the shared filesystem), as well as designing a parallel version for other architectures than computer clusters, such as GPGPU architectures.

References

1. Henzinger, T.A., Sifakis, J.: The embedded systems design challenge. In: FM. LNCS 4085 (2006) 1–15
2. Mari, F., Melatti, I., Salvo, I., Tronci, E.: Synthesis of quantized feedback control software for discrete time linear hybrid systems. In: CAV. LNCS 6174 (2010) 180–195
3. Tomlin, C., Lygeros, J., Sastry, S.: Computing controllers for nonlinear hybrid systems. In: HSCC. LNCS 1569 (1999) 238–255
4. Dean, J., Ghemawat, S.: Mapreduce: simplified data processing on large clusters. Commun. ACM **51**(1) (January 2008) 107–113
5. Lin, J., Dyer, C.: Data-Intensive Text Processing with MapReduce. Synthesis Lectures on Human Language Technologies. Morgan & Claypool Publishers (2010)
6. Rodriguez, M., Fernandez-Miaja, P., Rodriguez, A., Sebastian, J.: A multiple-input digitally controlled buck converter for envelope tracking applications in radiofrequency power amplifiers. IEEE Trans on Pow El **25**(2) (2010) 369–381
7. Kreisselmeier, G., Birkhölzer, T.: Numerical nonlinear regulator design. IEEE Trans. on Automatic Control **39**(1) (1994) 33–46
8. Bemporad, A., Giorgetti, N.: A sat-based hybrid solver for optimal control of hybrid systems. In: HSCC. LNCS 2993 (2004) 126–141
9. Della Penna, G., Magazzeni, D., Tofani, A., Intrigila, B., Melatti, I., Tronci, E.: Automated Generation of Optimal Controllers through Model Checking Techniques. Volume 15 of Lecture Notes in Electrical Engineering. Springer (2008)
10. Della Penna, G., Magazzeni, D., Mercorio, F., Intrigila, B.: UPMurphi: A tool for universal planning on pddl+ problems. In: ICAPS. (2009)
11. Schubert, W., Stengel, R.: Parallel synthesis of robust control systems. IEEE Trans. on Contr. Sys. Techn **6**(6) (1998) 701–706
12. Jurikovič, M., Čičák, P., Jelemenská, K.: Parallel controller design and synthesis. In: Proceedings of the 7th FPGAworld Conference. FPGAworld '10, New York, NY, USA, ACM (2010) 35–40

13. Pardey, J., Amroun, A., Bolton, M., Adamski, M.: Parallel controller synthesis for programmable logic devices. *Microprocessors and Microsystems* **18**(8) (1994) 451 – 457
14. Mari, F., Melatti, I., Salvo, I., Tronci, E.: Linear constraints as a modeling language for discrete time hybrid systems. In: ICSEA, IARIA (2012)
15. Alimguzhin, V., Mari, F., Melatti, I., Salvo, I., Tronci, E.: Automatic control software synthesis for quantized discrete time hybrid systems. In: CDC-ECE. (2012)
16. Alimguzhin, V., Mari, F., Melatti, I., Salvo, I., Tronci, E.: On model based synthesis of embedded control software. In: EMSOFT. (2012)
17. Mari, F., Melatti, I., Salvo, I., Tronci, E.: From boolean relations to control software. In: ICSEA. (2011)
18. Mari, F., Melatti, I., Salvo, I., Tronci, E.: Control software visualization. In: INFOCOMP, IARIA (2012)
19. Mari, F., Melatti, I., Salvo, I., Tronci, E.: Undecidability of quantized state feedback control for discrete time linear hybrid systems. In: ICTAC. LNCS 7521 (2012) 243–258
20. Fu, M., Xie, L.: The sector bound approach to quantized feedback control. *IEEE Trans. on Automatic Control* **50**(11) (2005) 1698–1711
21. Bryant, R.: Graph-based algorithms for boolean function manipulation. *IEEE Trans. on Computers* **C-35**(8) (1986) 677–691
22. Pacheco, P.: *Parallel Programming with MPI*. Morgan Kaufmann (1997)
23. So, W.C., Tse, C., Lee, Y.S.: Development of a fuzzy logic controller for dc/dc converters: design, computer simulation, and experimental evaluation. *IEEE Trans. on Power Electronics* **11**(1) (1996) 24–32
24. Kim, W., Gupta, M.S., Wei, G.Y., Brooks, D.M.: Enabling on-chip switching regulators for multi-core processors using current staggering. In: ASGI. (2007)
25. Lin, P.Z., Hsu, C.F., Lee, T.T.: Type-2 fuzzy logic controller design for buck dc-dc converters. In: FUZZ. (2005) 365–370